NANO LETTERS

2008
Vol. 8, No. 2
743−748

Geometric Confinement Governs the Rupture Strength of H-bond Assemblies at a Critical Length Scale

Sinan Keten and Markus J. Buehler*

Laboratory for Atomistic and Molecular Mechanics, Department of Civil and Environmental Engineering, Massachusetts Institute of Technology, 77 Massachusetts Avenue Room 1-272, Cambridge, Massachusetts

Received December 4, 2007; Revised Manuscript Received January 11, 2008

ABSTRACT

The ultrastructure of protein materials such as spider silk, muscle tissue, or amyloid fibers consists primarily of beta-sheets structures, composed of hierarchical assemblies of H-bonds. Despite the weakness of H-bond interactions, which have intermolecular bonds 100 to 1000 times weaker than those in ceramics or metals, these materials combine exceptional strength, robustness, and resilience. We discover that the rupture strength of H-bond assemblies is governed by geometric confinement effects, suggesting that clusters of at most 3–4 H-bonds break concurrently, even under uniform shear loading of a much larger number of H-bonds. This universally valid result leads to an intrinsic strength limitation that suggests that shorter strands with less H-bonds achieve the highest shear strength at a critical length scale. The hypothesis is confirmed by direct large-scale full-atomistic MD simulation studies of beta-sheet structures in explicit solvent. Our finding explains how the intrinsic strength limitation of H-bonds can be overcome by the formation of a nanocomposite structure of H-bond clusters, thereby enabling the formation of larger and much stronger beta-sheet structures. Our results explain recent experimental proteomics data, suggesting a correlation between the shear strength and the prevalence of beta-strand lengths in biology.

The mechanical behavior of biological structural protein materials under physiological or external stress conditions is exceedingly complex, partly due to the hierarchical architecture of these materials that extends from nano to macro.[1−5] Elasticity, strength, and the extreme toughness of these lightweight materials can be attributed to the nanostructure of their building blocks, which are single protein biomolecules that create filaments, fibrils, and fibers through self-assembly.

The strength of biological materials at the nanoscale is linked to protein unfolding, where the rupture of interstrand H-bonds primarily controls the mechanical resistance (Figure 1a illustrates the role of H-bonds in stabilizing key domains in the muscle tissue protein titin, Z1-Z2 telethonin complex and I27). Atomistic simulation[6,7] and single-molecule force spectroscopy studies[8−11] have shown that beta-sheet rich proteins exhibit particularly large rupture forces, because they employ parallel strands with numerous H-bonds that act as mechanical clamps under shear loading.[12−15] The unfolding behavior depends strongly on the pulling velocity, as discussed extensively in the literature.[16−18]

In earlier studies, the mechanical resistance of proteins has been linked to the orientation of beta-strand domains with respect to the applied load.[12−15] However, how the number of H-bonds in a strand (or equivalently, the strand

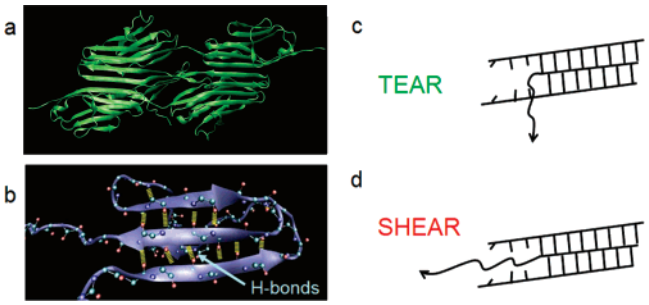

Figure 1. Molecular structure and loading conditions used for molecular dynamics simulations. Beta-sandwich structures are a characteristic feature of mechanical proteins, which employ networks of parallel H-bonds that work cooperatively in shear, like the Z1Z2-telethonin complex in titin (shown in panel a).[12−15] Interstrand H-bonds (thick yellow lines) act as mechanical clamps that resist unfolding, as shown in panel b for the I27 domain of titin. We consider a three-strand system with free chains at the ends, as shown in panel b, as a model to study the strength of beta-strands. We study two deformation modes: in-plane shear and out-of-plane shear, which we refer to as SHEAR and TEAR modes, respectively (panels c and d). In the TEAR mode, the middle strand is pulled out in the direction orthogonal to the strand direction. In the SHEAR mode, the middle strand is pulled in the direction of the beta-strand, leading to uniform loading of H-bonds.

* Corresponding author. E-mail: mbuehler@MIT.EDU. Phone: +1-617-452-2750. Fax: +1-617-258-6775.

10.1021/nl0731670 CCC: $40.75
Published on Web 02/13/2008

length), influences the strength remains divisive. There exist only phenomenological descriptions based on determining the energy barrier and the location of the transition state of mechanical unfolding pathways of proteins, extracted by studying the rate dependence of the mechanical unfolding force and the subsequent analysis with statistical theories. Furthermore, linking this information to deformation mechanisms and the specific rupture events in the context of the unfolding of complex protein structures remains unexplained. Similarly, although theoretical and experimental studies have provided great insight into the strength of multiple parallel H-bonds,[19−22] the coupling between elasticity of the protein backbone and the rupture mechanisms of H-bonds has not yet been clarified.

Despite significant advancements in our understanding of the nanomechanics of biological materials,[8−15] several key fundamental questions remains unanswered: What is the strength limit of H-bond assemblies, and how is it possible that protein materials such as spider silk or amyloids reach strengths that exceed those of steel, despite the weakness of H-bond interactions? Is there a physical explanation for the characteristic structure of beta-sheet protein domains, typically displaying ultrashort strand lengths with less than five residues, embedded in random coil protein domains?

As a simple model representation of larger beta-sheet rich protein structures (Figure 1a), we consider a small, full atomistic protein domain embedded in explicit solvent, as shown in Figure 1b. The model contains three beta-strands with interstrand H-bonds, representing the beta-sheet protein motif that forms larger protein structures, as shown in Figure 1a. The strands in our model system have free chains at their extremities, representing unraveled domains of a protein undergoing unfolding. In the first part of this paper, we model the behavior of this protein assembly by large-scale molecular dynamics (MD; for details of the MD approach see Supporting Information). In the analyses of the mechanical response of this system, we pull the center strand in different directions of loading, while the outermost strands remain fixed.

The goal of the computational experiments is to probe the strength and rupture mechanism of the model system in two extreme modes of deformation. In the out-of-plane shear mode (TEAR, Figure 1c), the middle strand is pulled perpendicular to the plane of the sheet. The computational experiment in the TEAR mode is designed so that the H-bonds break sequentially, one-by-one. This case enables us to assess the rupture behavior and energy landscape of individual H-bonds. We consider a second case, the in-plane shear mode (SHEAR, Figure 1d). Here, the middle strand is pulled out in the axial direction of the three strands. The SHEAR case is designed to assess the rupture behavior and the energy landscape of a large number of H-bonds under uniform shear loading. For both deformation modes TEAR and SHEAR, we carry out a systematic study of the rupture force F against pulling rate v, and plot the results on a logarithmic scale over 3 orders of magnitude (Figure 2a). The curves obtained for each deformation mode fall on two distinct lines in the F versus $\ln(v)$ plane. The Modified Bell

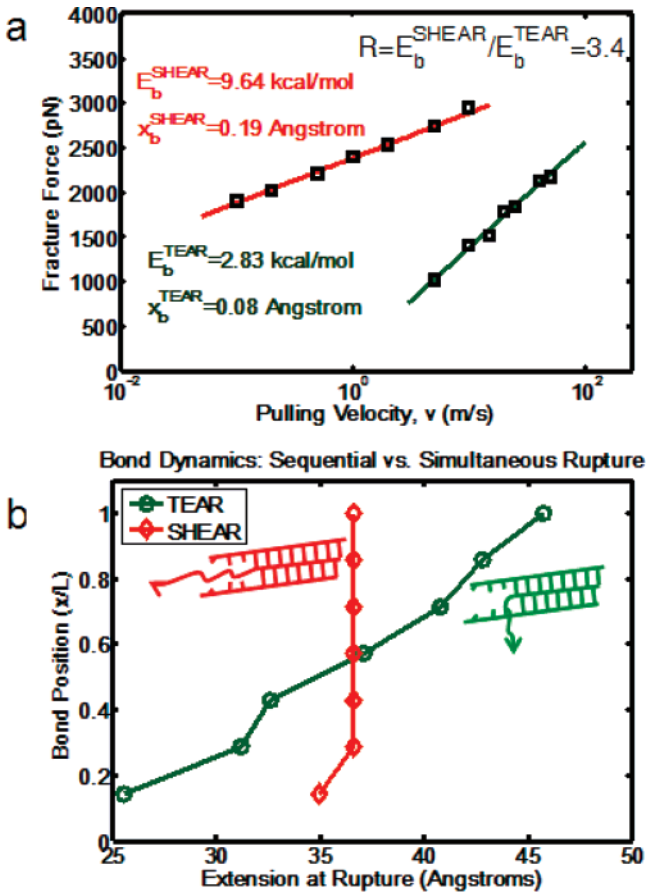

Figure 2. Unfolding force vs deformation speed, TEAR vs SHEAR deformation modes, and associated H-bond rupture mechanism (results of full atomistic molecular dynamics simulations in explicit water solvent). (a) Logarithmic relationship between the pulling speed and rupture force for both deformation modes. The parameters of the linear fit for each regime are used in conjunction with the modified Bell model to determine the energy landscape for each deformation mode. (b) The H-bond rupture dynamics, which reveals that the localization of strain in the TEAR mode leads to sequential rupture of H-bonds. In contrast, several H-bonds rupture concurrently in the SHEAR mode.

Theory (see Supporting Information and also ref 23) can be used to calculate discrete and unique values of the energy barrier to unfolding (E_b) for each deformation mode.

The energy barrier in the TEAR deformation mode is $E_b^{TEAR} = 2.83$ kcal/mol. An analysis of the bond rupture dynamics reveals that the H-bonds break sequentially (Figure 2b), indicating that the energy barrier to break a single H-bond in this protein is $E_{HB}^0 = 2.83$ kcal/mol. The energy barrier in the SHEAR deformation mode is $E_b^{SHEAR} = 9.64$ kcal/mol, significantly larger than in the TEAR mode. The analysis of the rupture mechanism in the SHEAR mode reveals that H-bonds break in clusters of multiple bonds (Figure 2b).

The comparison of the energy barriers in the TEAR and SHEAR mode enables us to calculate how many H-bonds participate in the rupture process under SHEAR loading. This is possible because the energy barrier in the TEAR mode corresponds to rupture of individual H-bonds. The number of H-bonds that break concertedly in the SHEAR mode is given by the ratio of the E_b values for SHEAR and TEAR;

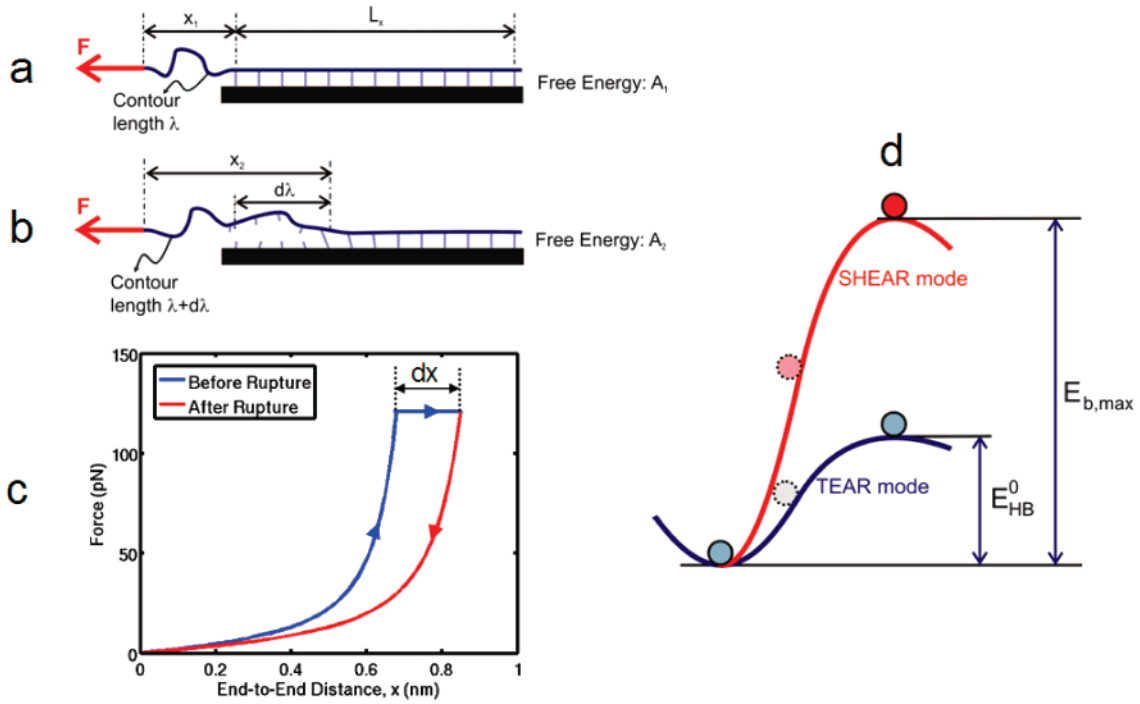

Figure 3. Schematics to explain the main concepts of the WLC-based fracture theory, as well as the implications on the energy landscape. (a) We consider a single double-strand system as a polypeptide chain of infinite length ($L_x \rightarrow \infty$) with a free end of length a. The polypeptide chain is stabilized by an array of parallel H-bonds, and strained due to the external force F. At the onset of rupture (panel b), several H-bonds break, and the contour length increases due to the detachment of a piece of the chain of length $d\lambda$. (c) The change in the contour length and the end-to-end distance at the onset of rupture yields two distinct WLC curves, relating to the states before and after rupture; the area enclosed between the WLC force extension curves is equivalent to the change in free energy before and after rupture. This dissipated (released) energy must equal the adhesion energy per unit length at the onset of rupture. (d) A schematic of how the energy barrier changes from rupture of a single H-bond up until the limiting energy barrier $E_{b,max}$, when 3−4 H-bonds rupture simultaneously. This energy barrier is the highest energy barrier of an assembly of H-bonds under uniform loading.

it is $E_b^{SHEAR}/E_b^{TEAR} \approx 3.4$. This suggests that H-bonds break in clusters of 3−4 but not more even when the loading conditions (uniform shear) allow them to respond cooperatively.

This is a significant finding. Despite the presence of more than a dozen H-bonds in the system and all loaded in uniform shear, H-bond rupture occurs in clusters of 3−4. In terms of the energy barrier, it appears to be limited to a finite value, despite the possibility for a manifold increase of the resulting energy barrier due to the large number of H-bonds.

We propose a theoretical model based on thermodynamical fracture mechanics to provide an explanation for this phenomenon. We consider a simple model as shown in Figure 3a, where a polypeptide chain of length L_x is attached to a substrate via H-bonds, strained by a force F, applied at the free end of the protein. This model, which is a simplistic representation of a single shear-loaded beta-strand stabilized by H-bonds, is part of a larger protein domain. Because we seek a maximum strength value that is not hindered by too few H-bonds, we consider an infinitely long beta-strand (the length of the strand $L_x \rightarrow \infty$; see Figure 3a for the geometry).

We ask the question, what is the unfolding rupture force and the rupture mechanism of such a large assembly of H-bonds loaded in shear in the asymptotic thermodynamical long-time limit? We proceed in two steps. First, we calculate the asymptotic strength limit of an assembly of H-bonds. Second, we calculate how many H-bonds participate in the unit rupture event.

We begin with a calculation of the quasi-static, asymptotic strength limit for an assembly of H-bonds loaded in shear, by adopting Griffith's theory of fracture mechanics for nanoscale phenomena.[24−26] The onset of failure is characterized by the condition that the change in free energy W_P due to the extension of the fracture balances the energy necessary to create new surfaces, γ_s (the parameter γ_s is the one dimensional equivalent of surface energy and is defined as $\gamma_s = E_{HB}^0/L_{x,0}$, where E_{HB}^0 is the energy required to rupture a single H-bond, and $L_{x,0}$ is the distance between two H-bonds). The negative of the expression for the free energy change with respect to a rupture advance of one unit distance, δa, is called the energy release rate $G = -\delta W_P/\delta a$. This leads to

$$G = -\frac{\delta W_P}{\delta a} \stackrel{!}{=} \gamma_s \qquad (1)$$

At the force levels of interest, the elasticity of the free end of the protein backbone is primarily governed by entropic (rather than energetic) effects. The Marko−Siggia wormlike chain (WLC) model[27] is a widely used approach to describe the entropic elasticity of polypeptide chains and is adopted here as the elastic description of the backbone (a wide range

of earlier studies provide substantial evidence that the WLC theory is an appropriate model for the elastic behavior of individual, unconstrained polypeptide chains[9,11,28,29]).

We seek an expression of how the free energy changes as a function of rupture extension, considering the WLC model to describe the elasticity of the protein backbone. Figure 3c schematically illustrates the process of loading the structure, the rupture event, and the return to the initial configuration. The area between the two curves is the dissipated free energy that is employed in the breaking of the H-bonds, according to eq 1.

The approach is derived in full detail in the Supporting Information. We find that the energy release rate $G(\alpha) = k_B T/(4\xi_p)(\alpha(1-\alpha)^{-2} - (1-\alpha)^{-1} + 2\alpha^2 - 1)$, depending solely on the parameter $\alpha = x_1/\lambda_1$ (α is the ratio of end-to-end length of the free chain to its contour length and is defined in the range from 0 to 1; see Figure 3a,b). This equation is used to calculate α_{cr} that satisfies eq 1. The asymptotic strength limit is then

$$F_{break}(\alpha_{cr}) = \frac{k_B T}{4\xi_p}[(1-\alpha_{cr})^{-2} + 4\alpha_{cr} - 1] \qquad (2)$$

Now we calculate the number of H-bonds that participate in a unit fracture event. We consider the process at the rupture front at the moment when an unknown number of N_{cr} H-bonds break. We model the strength of this cluster of H-bonds by a statistical theory based on Bell's original model.[23] The key parameter is the energy barrier. The energy barrier rises N_{cr}-fold when N_{cr} H-bonds break simultaneously. Thus the rupture force of this system is

$$F^{local}_{break}(N_{cr}) = \frac{1}{x_B}\left[k_B T \ln\left(\frac{1}{\omega\tau}\right) + E^0_{HB} N_{cr}\right] \qquad (3)$$

where $\omega = 1 \times 10^{13}$ 1/s (natural frequency of bond vibration), τ is the characteristic time scale for H-bond dissociation, and x_B is the applied pulling distance at the moment of bond rupture. The parameter $x_B = 4$ Å due to the geometry of the beta-strand, and the characteristic time scale $\tau = 20$ ps (τ corresponds to the time scale at which H-bond rupture occurs; this characteristic time scale of H-bond rupture is chosen according to experimental[30] and computational[17] results and characterizes the dynamics of H-bond rupture, which is much faster than the applied loading in the asymptotic limit).

At the moment of rupture, the local rupture force given by eq 3 must equal the critical rupture load F_{break} given by eq 2. Setting $F^{local}_{break}(N_{cr}) = F_{break}$ thus enables us to calculate the number of H-bonds that break simultaneously in the unit rupture event

$$N_{cr} = \frac{k_B T}{E^0_{HB}}\left[\frac{x_b}{4\xi_p}[(1-\alpha_{cr})^{-2} + 4\alpha_{cr} - 1] - \ln\left(\frac{1}{\omega\tau}\right)\right] \qquad (4)$$

A schematic overview over the entire derivation is shown in Supporting Information, Figure S1; Supporting Information, Table 1 provides an overview over all variables used here.

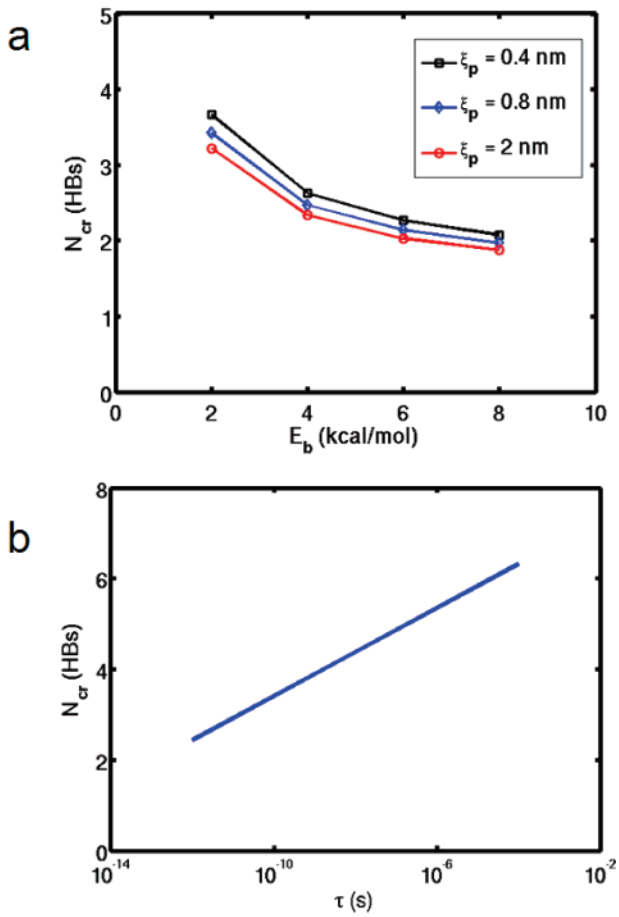

Figure 4. Sensitivity analysis for the critical number of H-bonds, N_{cr}, as a function of key parameters in the system. (a) We plot N_{cr} as a function of E_b and ξ_p and show that $N_{cr} \approx 3 \pm 1$ H-bonds over the domain of a range of measured values for variations in the H-bond energy and for variations in the persistence length. (b) There is a rather weak logarithmic dependence of N_{cr} on the characteristic time of H-bond rupture, τ. The critical number of H-bonds $N_{cr} \approx 4 \pm 2$ H-bonds over 8 orders of magnitude of time scale (here we use $E_b = 2.83$ kcal/mol and $\xi_p = 0.4$ nm). These results illustrate the significance and universality of our finding and support that the results reported here are very robust.

We present the variation in the value of N_{cr} due to variations in the parameters ξ_p, E^0_{HB}, and τ in Figure 4. These results suggest that our prediction is very robust with respect to changes in the input parameters.

The specific beta-sheet molecular dynamics study discussed in this letter represents a specific numerical example that illustrates the validity of our theory. To obtain a numerical prediction for N_{cr} for this system, we choose $T = 300$ K and $\gamma_s = 0.94$ kcal·mol^{-1} Å^{-1} (for $E^0_{HB} = 2.83$ kcal/mol from the TEAR mode MD simulation) and $\xi_p = 0.4$ nm from previous experimental studies.[8,11,30] The prediction of the critical number of H-bonds that break concurrently is $N_{cr} = 3.1$. The corresponding predicted maximum energy barrier for this case is $E_{b,max} = N_{cr}E^0_{HB} = 8.77$ kcal/mol with an asymptotic strength limit (at vanishing pulling rates) of 96 pN.

This is the most important result of this paper. The value $E_{b,max} = N_{cr}E^0_{HB}$ represents the highest energy barrier that can be achieved by a uniformly loaded H-bond assembly,

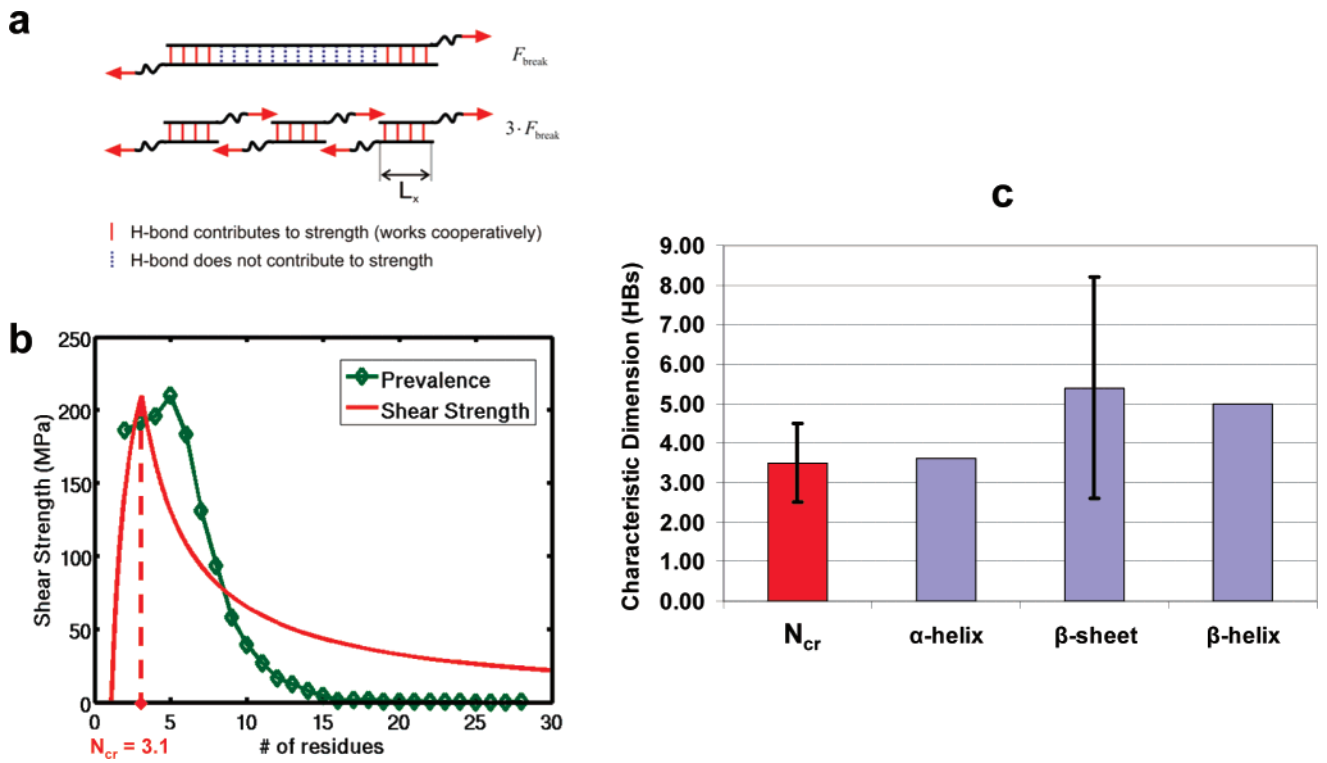

Figure 5. Size effects, shear strength, and prevalence of strand length of beta-sheets. (a) This plot illustrates the difference of the strength of a single, long beta strand vs a combination of multiple small strands. In the upper plot, only H-bonds at the boundary participate in the rupture process and provide resistance. In the lower plot, all H-bonds throughout the entire structure contribute to the strength, making the overall structure three times stronger. (b) Shear strength of beta-sheets as a function of strand length and the prevalence of beta-sheet strand length (experimental prevalence data taken from ref 31). The highest shear resistance is found at a characteristic length scale of 3.1 residues (see Supporting Information for shear strength calculation). Beyond this length scale, the shear strength drops rapidly. The plot of the prevalence over the strand length illustrates that shorter beta-strands are more prevalent;[31] in particular, strands that employ less than five residues are most common, and the prevalence decays sharply after this point. (c) Comparison of the characteristic dimensions of H-bond assemblies loaded in parallel in alpha-helices, beta-sheets, and beta-helices with our prediction. In conjunction with our theoretical prediction, this plot suggests that geometric confinement may be a universal strategy to create particularly stable protein structures as fundamental material building blocks.

providing an upper limit for its strength. Moreover, the prediction for the energy barrier is very close to what is observed in the SHEAR mode ($E_b^{SHEAR} = 9.64$ kcal/mol $\approx$ $E_{b,max} = 8.77$ kcal/mol) in MD simulations. There exists an intrinsic upper limit of 3−4 H-bonds that can break concurrently, illustrating that the conventional assumption of uniform shear loading of H-bonds in beta-strand fails once the number of H-bonds in an assembly exceeds this critical value.

Figure 3d shows a schematic that depicts the energy barriers of a single H-bond, as well as the limiting value $E_{b,max}$ that corresponds to the SHEAR and TEAR modes. We note that the particular geometry of the H-bond assembly is irrelevant in the theoretical derivation, in particular, whether or not the H-bonds are arranged in a three-strand system or in a two-strand system in a beta-sheet. Theory predicts the critical number of H-bonds that can break concurrently under any assembly geometry that allows uniform deformation of multiple bonds.

The fact that the results of this model only depend on fundamental, "first-principles" properties of protein structures underlines the significance of our finding. The only input parameters in this model are the persistence length ξ_p of the polypeptide chain, as well as the dissociation energy of a H-bond, E_{HB}^0 (γ_s is calculated directly from E_{HB}^0). Both parameters can be determined reliably from either experiment or atomistic simulation.

Because the number of H-bonds in a beta-strand is proportional to the number of residues ($L_{cr} \sim N_{cr}$, assuming that the H-bonds are arranged in a linear geometry as shown in Figure 5a), this result leads to a critical geometric strand length L_{cr}. Strands beyond L_{cr} are prone to localization of deformation and rupture of H-bonds that reduces their efficacy, because not all of the H-bonds participate in the rupture process and thus contribute to the strength (Figure 5a). The physical basis for this limitation is the entropic elasticity of the protein backbone (an intrinsic property of protein structures), as well as the characteristic energy of H-bonds (also an intrinsic property of protein structures).

Notably, this finding explains recent proteomics data[31] obtained by analyzing the strand lengths of a wide range of beta-sheet structures. Figure 5b illustrates that shorter beta-strands are more prevalent;[31] strands that employ less than five residues are very common, and the prevalence decays sharply after this point. Further, we find that the shear strength correlates closely to the prevalence of the strand length (see Figure 5b). The key conclusion of this analysis is that the evolutionary driving force for the selection of

strand lengths in beta-sheet structures may be the maximization of the mechanical (and hence, thermodynamical) stability. This hypothesis is strongly supported by the fact that both the prevalence curve and the shear strength prediction show a very similar trend when plotted against strand length (Figure 5b).

Moreover, the theoretical development reported here is not limited to beta-strands. As long as the system of interest contains an assembly of H-bonds that are loaded uniformly, the theoretical derivation reported here is valid. Thus, our finding may also explain the characteristic structure of alpha-helical proteins, which feature 3.6 H-bonds per turn, which are loaded in parallel and that break concertedly (as recently shown in ref 17). The characteristic number of H-bonds per turn in alpha-helices closely resembles the strength limit reported here. In other words, increasing the number of H-bonds per turn does not have an effect in increasing the mechanical stability of the protein. Similarly, beta-helix protein structures also feature a helical arrangement of ultra-short beta-strand segments with each less than five H-bonds. Figure 5c shows a quantitative comparison of the characteristic dimensions of several protein structures discussed above with the characteristic number of H-bonds reported here.

The intrinsic strength limit of H-bond assemblies can only be overcome by using structural hierarchies, that is, formation of assemblies of structures that each contain confined beta-strands mingled with entropic domains (e.g., see Figure 5a). Indeed, such hierarchical structures are commonly found in many mechanically strong biological materials such as spider silk, cytoskeletal proteins, or muscle tissue.

Our results may lay the foundation for development of plasticity and strength models for protein materials. Models such as the one presented here provide valuable insight for designing mechanically robust and strong self-assembling peptide-based materials.

A variety of models for the fracture mechanics of ceramics and metals have been reported over the past decades, involving detailed descriptions of dislocations, plasticity, and crack extension mechanisms.[26,32,33] However, similar advances for biological protein materials have thus far remained elusive. In analogy to dislocation nucleation and propagation in ductile metals, the breaking of H-bonds represents a fundamental unit mechanism of failure in protein materials. To the best of our knowledge, this paper for the first time describes a rigorous fracture mechanics based approach to describe the fundamental bond rupture events in protein materials.

Acknowledgment. S.K. acknowledges support by the Presidential Graduate Fellowship Program at the Massachusetts Institute of Technology. The authors acknowledge a supercomputing grant at the San Diego Supercomputing Center (SDSC). This research was supported by the Army Research Office (ARO), Grant W911NF-06-1-0291 (program officer Dr. Bruce LaMattina), by a National Science Foundation CAREER Award, Grant CMMI-0642545 (program manager Dr. Jimmy Hsia), as well as the Solomon Buchsbaum AT&T Research Fund. The authors declare no conflict of interest.

Supporting Information Available: The materials and methods section including the full derivation of the theoretical approaches, as well as a description of the computational procedure. Supporting figure and tables for explaining theoretical considerations and supporting references have also been provided. This material is available free of charge via the Internet at http://pubs.acs.org.

References

(1) Lakes, R. *Nature* **1993**, *361* (6412), 511−515.
(2) Wegst, U. G. K.; Ashby, M. F. *Philos. Mag.* **2004**, *84* (21), 2167−2181.
(3) Aizenberg, J.; Weaver, J. C.; Thanawala, M. S.; Sundar, V. C.; Morse, D. E.; Fratzl, P. *Science* **2005**, *309* (5732), 275−278.
(4) Arzt, E.; Gorb, S.; Spolenak, R. *Proc. Natl. Acad. Sci. U.S.A.* **2003**, *100* (19), 10603−10606.
(5) Buehler, M. J. *Proc. Natl. Acad. Sci. U.S.A.* **2006**, *103* (33), 12285−12290.
(6) Lu, H.; Schulten, K. *Biophys. J.* **2000**, *79* (1), 51−65.
(7) Lee, E. H.; Gao, M.; Pinotsis, N.; Wilmanns, M.; Schulten, K. *Structure* **2006**, *14* (3), 497−509.
(8) Rief, M.; Gautel, M.; Oesterhelt, F.; Fernandez, J. M.; Gaub, H. E. *Science* **1997**, *276* (5315), 1109−1112.
(9) Rief, M.; Gautel, M.; Schemmel, A.; Gaub, H. E. *Biophys. J.* **1998**, *75* (6), 3008−3014.
(10) Rief, M.; Pascual, J.; Saraste, M.; Gaub, H. E. *J. Mol. Biol.* **1999**, *286* (2), 553−561.
(11) Oberhauser, A. F.; Marszalek, P. E.; Erickson, H. P.; Fernandez, J. M. *Nature* **1998**, *393* (6681), 181−185.
(12) Brockwell, D. J.; Paci, E.; Zinober, R. C.; Beddard, G. S.; Olmsted, P. D.; Smith, D. A.; Perham, R. N.; Radford, S. E. *Nat. Struct. Biol.* **2003**, *10* (9), 731−737.
(13) Grater, F.; Shen, J.; Jiang, H.; Gautel, M.; Grubmuller, H. *Biophys. J.* **2005**, *88* (2), 790−804.
(14) Rohs, R.; Etchebest, C.; Lavery, R. *Biophys. J.* **1999**, *76* (5), 2760−2768.
(15) West, D. K.; Brockwell, D. J.; Olmsted, P. D.; Radford, S. E.; Paci, E. *Biophys. J.* **2006**, *90* (1), 287−297.
(16) Sotomayor, M.; Schulten, K. *Science* **2007**, *316* (5828), 1144−1148.
(17) Ackbarow, T.; Chen, X.; Keten, S.; Buehler, M. J. *Proc. Natl. Acad. Sci. U.S.A.* **2007**, 0705759104.
(18) Hyeon, C.; Thirumalai, D. *J. Phys.: Condens. Matter* **2007**, *19* (11) 113101.
(19) Seifert, U. *Phys. Rev. Lett.* **2000**, *84* (12), 2750−2753.
(20) Erdmann, T.; Schwarz, U. S. *Phys. Rev. Lett.* **2004**, *92* (10) 108102.
(21) Heymann, B.; Grubmuller, H. *Phys. Rev. Lett.* **2000**, *84* (26), 6126−6129.
(22) Evans, E.; Ritchie, K. *Biophys. J.* **1997**, *72* (4), 1541−1555.
(23) Bell, G. I. *Science* **1978**, *200* (4342), 618−627.
(24) Griffith, A. A. *Philos. Trans. R. Soc. London, Ser. A* **1921**, (221), 163−168.
(25) Buehler, M. J.; Gao, H. J. *Nature* **2006**, *439* (7074), 307−310.
(26) Broberg, K. B. *Cracks and Fracture*; Academic Press: New York, 1990.
(27) Marko, J. F.; Siggia, E. D. *Macromolecules* **1995**, *28* (26), 8759−8770.
(28) Bustamante, C.; Smith, S. B.; Liphardt, J.; Smith, D. *Curr. Opin. Struct. Biol.* **2000**, *10* (3), 279−285.
(29) Buehler, M. J.; Wong, S. Y. *Biophys. J.* **2007**, *93* (1), 37−43.
(30) Sheu, S. Y.; Yang, D. Y.; Selzle, H. L.; Schlag, E. W. *Proc. Natl. Acad. Sci. U.S.A.* **2003**, *100* (22), 12683−12687.
(31) Penel, S.; Morrison, R. G.; Dobson, P. D.; Mortishire-Smith, R. J.; Doig, A. J. *Protein Eng.* **2003**, *16* (12), 957−961.
(32) Hirth, J. P.; Lothe, J. *Theory of Dislocations*; Wiley-Interscience: New York, 1982.
(33) Buehler, M. J.; Ackbarow, T. *Mater. Today* **2007**, *10* (9), 46−58.

NL0731670